PHYSICAL REVIEW B VOLUME 57, NUMBER 10 1 MARCH 1998-II

Antiferromagnetic metallic state in doped manganites

T. Akimoto, Y. Maruyama, Y. Moritomo,* and A. Nakamura
Center for Integrated Research in Science and Engineering (CIRSE), and Department of Applied Physics, Nagoya University, Nagoya 464-01, Japan

K. Hirota
Department of Physics, Tohoku University, Sendai 980-77, Japan

K. Ohoyama and M. Ohashi
Institute for Materials Research, Tohoku University, Sendai 980-77, Japan

(Received 6 January 1998)

Electronic and magnetic properties are systematically investigated for doped manganites $R_{1-x}Sr_xMnO_3$ ($R=La_{1-z}Nd_z$) by changing the nominal hole concentration x and the averaged ionic radius of the perovskite A site (z), or the one-electron bandwidth W. In the heavily doped region ($x \geqslant 0.50$), we observed a layered-type (A-type) antiferromagnetic state with metallic conductivity ($\rho \approx 4\times10^{-4}$ Ω cm at 5 K for $La_{0.46}Sr_{0.54}MnO_3$). This observation suggests that the antiferromagnetic metallic (AFM) state is the alternative ground state for doped manganites, besides the ferromagnetic metallic (FM) state. [S0163-1829(98)51610-4]

The recent observation of colossal magnetoresistance[1] (the CMR effect) in the doped manganites has sparked a great amount of effort to understand the unusual electronic and magnetic properties of these materials. The most commonly studied manganites $R_{1-x}A_xMnO_3$, where R and A are the trivalent rare-earth and divalent alkaline-earth ions, respectively, have the distorted perovskite structure with three-dimensional networks of the MnO_6 octahedra. Its generic behavior of paramagnetic-to-ferromagnetic transition is understood within the framework of the double-exchange (DE) theory,[2–4] which includes only the transfer integral t of the e_g electrons and the on-site exchange interaction (Hund's-rule coupling; J_H) between the itinerant e_g electrons and localized t_{2g} spins ($S=3/2$). To explain the colossal value of the MR for the system having small W, e.g., $La_{1-x}Ca_xMnO_3$,[5] however, we need additional mechanisms for carrier localization above T_C as well as magnetic field release of the localization. Perhaps the most probable mechanism to supplement the DE model is the polaron formation originating from the Jahn-Teller (JT) instability of the MnO_6 octahedra.[6]

The doped manganites show much more multifarious properties in the heavily doped region ($x \geqslant 0.5$). In the case of $La_{1-x}Ca_xMnO_3$,[5,7] the ground state changes with hole doping beyond $x \sim 0.5$ from the ferromagnetic metallic (FM) state to an antiferromagnetic insulating (AFI) state. Ramirez *et al.*[7] insisted that the FM state and the charge-ordered state located above the AFI state are the essential cooperative states governed by the Hund's-rule coupling (J) and the JT energies. Recently, Kawano *et al.*[8] have performed the neutron-diffraction measurements on $Pr_{1-x}Sr_xMnO_3$ ($x=0.50$) and $Nd_{1-x}Sr_xMnO_3$ ($x=0.55$), and found that these compounds exhibit a layered-type (A-type) antiferromagnetic spin-ordering, similar to the parent $LaMnO_3$.

In this paper, we have investigated the electronic and magnetic properties for $(La_{1-z}Nd_z)_{1-x}Sr_xMnO_3$, especially for the heavily doped region, by changing the doping level x and the averaged ionic radius (z). We can reduce the one-electron bandwidth W by partially substituting the smaller Nd^{3+} ions for the larger La^{3+} ions (increasing z; *chemical pressure*).[9] Even in the $La_{1-x}Sr_xMnO_3$ system with maximal W, further hole doping ($x \geqslant 0.54$) is found to alter the ground state from the FM state to the A-type antiferromagnetic state. Surprisingly, the compound remains metallic ($\rho \approx 4\times10^{-4}$ Ω cm at 5 K) even below $T_N(=200\ \mathrm{K})$, indicating that the ground state is an *antiferromagnetic metallic* (AFM) state. The AFM state is found to be distributed over the wide $x-z$ region adjacent to the FM state, indicating that the state is another ground state for the doped manganites. We discuss the AFM state in terms of the anisotropy of the e_g orbitals.

Crystals of $(La_{1-z}Nd_z)_{1-x}Sr_xMnO_3$ [$(x,z)=(0.40,\ 1.0)$, $(0.44, 1.0)$, $(0.46, 0.6)$, $(0.46, 0.8)$, $(0.48, 1.0)$, $(0.50, 0.0)$, $(0.50, 1.0)$, $(0.52, 1.0)$, $(0.54, 0.0)$, $(0.54, 0.2)$, $(0.54, 0.4)$, $(0.54, 0.8)$, $(0.54, 1.0)$, $(0.56, 1.0)$, $(0.57, 0.0)$, $(0.60, 0.0)$ and $(0.60, 1.0)$] were grown by the floating-zone method at a feeding speed of 7–9 mm/h. A stoichiometric mixture of commercial La_2O_3, Nd_2O_3, $SrCO_3$, and Mn_3O_4 powder was ground and calcined two times at 1350 °C for 24 h. Then, the resulting powder was pressed into a rod with a size of 5 mm $\phi \times 60$ mm and sintered at 1350 °C for 48 h. The ingredient could be melted congruently in a flow of O_2. Large crystals, typically 4 mm in diameter and 20 mm in length, were obtained. Powder x-ray-diffraction measurements at room temperature and Reitveld analysis[10] indicate that the crystals were almost single phase. A small amount of $SrMnO_3$ impurity phase, however, is inevitably introduced to the melt-grown crystal ingot, especially for the higher-x samples. Except for $La_{0.5}Sr_{0.5}MnO_3$ ($x=0.50$, $z=0.0$),[9] the crystal symmetry is orthorhombic ($Pbnm$; $Z=4$).

We show in Fig. 1 temperature dependence of resistivity ρ and magnetization M for crystals of $La_{1-x}Sr_xMnO_3$ ($z=0.0$) at $x=0.50$ and 0.54. For four-probe resistivity measurements, the crystal was cut into a rectangular shape, typi-

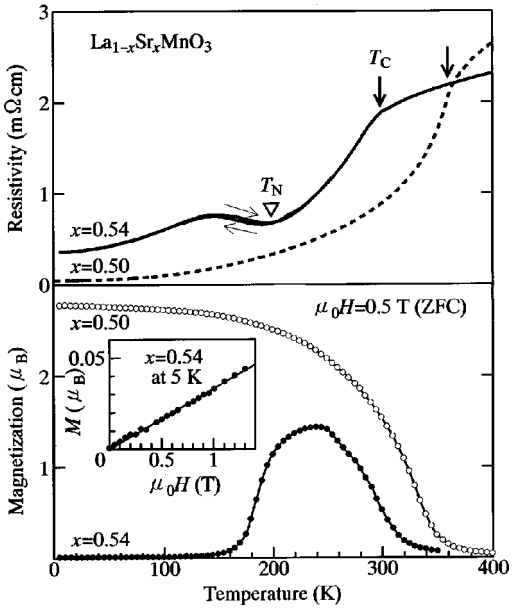

FIG. 1. Temperature dependence of resistivity (upper panel) and magnetization (lower panel) for crystals of $La_{1-x}Sr_xMnO_3$. Solid curves are for $x=0.54$ and broken curves for $x=0.50$. Arrows and triangles represent the Curie temperatures (T_C) and Néel temperatures (T_N), respectively. Inset shows magnetization curve at 5 K for $x=0.54$.

cally of $3\times1\times0.5$ mm^3, and electrical contacts were made with a heat-treatment-type silver paint. M was measured under a field of $\mu_0 H=0.5$ T after cooling down to 5 K in zero field (ZFC) using a superconducting quantum interference device (SQUID) magnetometer. Curie temperature T_C was determined from the inflection point of the $M-T$ curve. At $x=0.50$, the $\rho-T$ curve steeply decreases below T_C ($=360$ K; downward arrow) down to $\sim5\times10^{-5}$ Ω cm at 5 K. By contrast, the $x=0.54$ compound shows a ferromagnetic-to-antiferromagnetic transition at $T_N=200$ K (see the lower panel of Fig. 1), accompanying a slight increase of the ρ value. Nevertheless, the resistivity for $x=0.54$ remains low ($\sim4\times10^{-4}$ Ω cm at 5 K) even in the antiferromagnetic phase, indicating that the hole-doping procedure beyond $x\sim0.5$ alters the ground state for $La_{1-x}Sr_xMnO_3$ from the FM state to the AFM state. A similar AFM state is observed also for $x=0.57$ (not shown). For $x=0.60$, however, the ρ value steeply increases below $T_N=250$ K.

To investigate the spin structure for the AFM state, neutron-diffraction measurements were performed with a high-efficiency powder diffractometer with a 150-detector system, HERMES, installed at the JRR-3M reactor in Japan Atomic Energy Research Institute, Tokai, Japan. Neutrons with wavelength 1.819 Å were obtained by the (331) reflection of a Ge monochromator, and a combination of 12′-Blank-Sample-18′ collimator. Melt-grown crystal ingots were crushed into fine powder and sealed in a vanadium capsule with helium gas, and mounted at the cold head of the closed-cycle He-gas refrigerator. The nuclear Bragg reflections in the paramagnetic state (330 K) are well reproduced with the orthorhombic structure ($Pbnm$; $Z=4$) with lattice constants of $a=5.4329(7)$ Å, $b=5.4470(8)$ Å, and $c=7.7556(9)$ Å. Figure 2 shows the powder pattern for

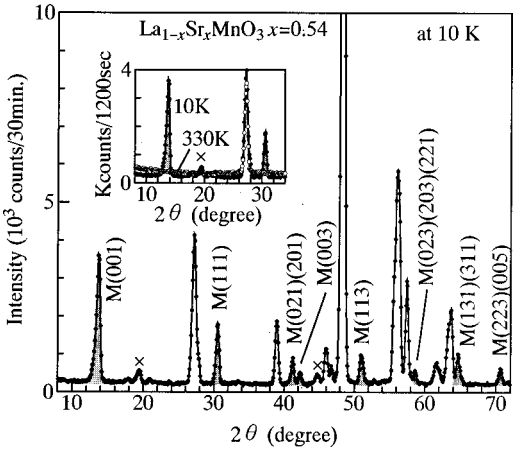

FIG. 2. Neutron powder profiles for $La_{0.46}Sr_{0.54}MnO_3$ ($x=0.54$) at 10 K. Shaded areas indicate magnetic superlattice reflections, which are indexed in the $Pbmn$ setting. Inset shows temperature dependence of the powder neutron profiles: open and closed circles are at 330 K ($>T_C$) and at 10 K ($<T_N$). Small impurity peaks (cross) are originated hexagonal $SrMnO_3$.

$La_{0.46}Sr_{0.54}MnO_3$ ($x=0.54$, $z=0.0$) in the antiferromagnetic phase at 10 K. The observed magnetic superlattice reflections (indicated by hatching) can all be indexed by the A-type antiferromagnetic structure.[11] A similar spin ordering has been reported for $Nd_{0.45}Sr_{0.55}MnO_3$ ($x=0.55$, $z=1.0$),[8] suggesting that the A-type structure is one of the most stable magnetic structures for the doped manganites.

Now, let us proceed to the lattice effect on the AFM state. Figure 3 shows the $\rho-T$ curves for $(La_{1-z}Nd_z)_{0.46}Sr_{0.54}MnO_3$ ($x=0.54$) with various z values. The $\rho-T$ curves were obtained in the cooling run. Downward arrows and open triangles represent T_C and T_N, respec-

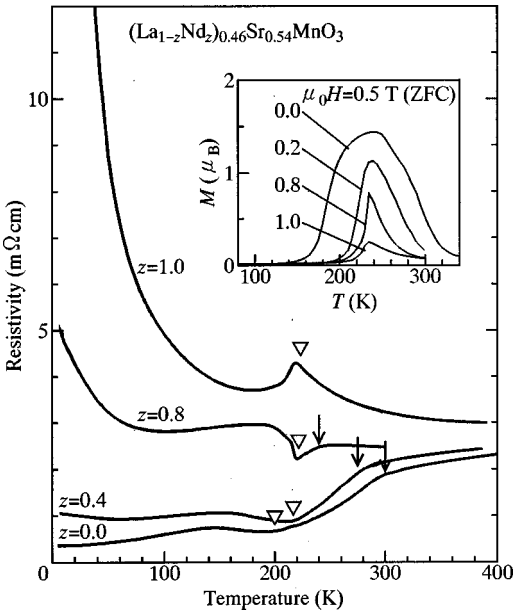

FIG. 3. Resistivity curves for crystals of $(La_{1-z}Nd_z)_{0.46}Sr_{0.54}MnO_3$ ($x=0.54$). Arrows and triangles represent the Curie temperatures (T_C) and Néel temperatures (T_N), respectively. Inset shows magnetization M under a field of $\mu_0 H=0.5$ T after cooling down to 5 K in zero field (ZFC).

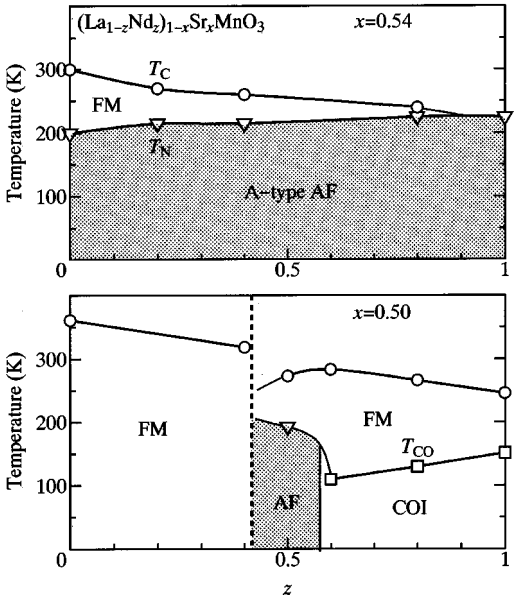

FIG. 4. Upper panel: electronic phase diagram for $(La_{1-z}Nd_z)_{0.46}Sr_{0.54}MnO_3$ ($x=0.54$). Lower panel: phase diagram for $x=0.50$ [$(La_{1-z}Nd_z)_{0.50}Sr_{0.50}MnO_3$] cited from Ref. 9. T_C, T_N, and T_{CO} represent Curie, Néel and charge-ordering temperatures, respectively. FM, AF, and COI means ferromagnetic metallic, antiferromagnetic, and charge-ordering insulating states, respectively. Vertical broken line in the lower panel is the structural phase boundary between the rhombohedral ($R3c$; $z\leqslant 0.4$) and orthorhombic ($Pbmn$; $z>0.4$) ones.

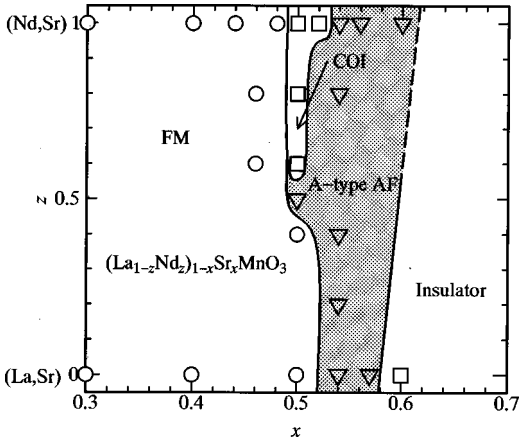

FIG. 5. Ground states for $(La_{1-z}Nd_z)_{1-x}Sr_xMnO_3$ as a function of the doping level x and the one-electron bandwidth W (or z). $(x,z)=(0.30,\ 0.0)$ and $(0.40,\ 0.0)$ are cited from Ref. 12. Circles, triangles, and squares represent the ferromagnetic metallic (FM), antiferromagnetic (AF), and insulating ground states, respectively. COI means charge-ordering insulating state.

tively (see also the $M-T$ curves in the inset). With increasing z (decreasing W), the reduced carrier itineracy suppresses the DE interaction and hence T_C, and eventually the FM state disappears above $z=0.8$. The $\rho-T$ curve below $z=0.8$ shows a metallic behavior in the antiferromagnetic phase, except for the low-temperature region ($\leqslant 60$ K) where weak localization effect is observed. In the case for $z=1.0$, the curve shows a semiconducting behavior though the magnitude of ρ remains low ($\sim 10^{-1}\Omega$ cm at 5 K).[12] The less-itinerant carriers, which cannot contribute to the macroscopic charge transport, can mediate the ferromagnetic DE interaction in a bond-percolative manner. (An insulating but ferromagnetic state exists near the insulator-to-metal phase boundary for $La_{1-x}Sr_xMnO_3$.[13]) A similar antiferromagnetic state is observed for $(La_{0.5}Nd_{0.5})_{0.5}Sr_{0.5}MnO_3$ ($x=0.5$ and $z=0.5$) (Ref. 9) and for $Pr_{0.5}Sr_{0.5}MnO_3$.[8,14] Here we have found that the metallic conductivity remains down to the lowest temperature for the large-W compound ($z\leqslant 0.4$) even with the A-type spin structure. This suggests that the layered-type spin ordering is originated in the DE mechanism mediated by the mobile e_g electrons.

Thus obtained T_C and T_N for $x=0.54$ are plotted with circles and triangles in the upper panel of Fig. 4 as a function of z (or W). The apparent suppression of T_N with decreasing z (or increasing W) is due to the FM phase located at the high-temperature side, which suppresses the competing A-type AF state. In the whole z region, the ground state is the A-type AF state. Especially, the resistivity remains metallic ($d\rho/dT\geqslant 0$) down to the lowest temperature in the large-W region ($z\leqslant 0.4$). A similar highly-conductive AF state is observed for $x=0.50$ (lower panel; cited from Ref. 9), even though the diagram is complicated partly due to the structural transition from rhombohedral ($R3c$; $z<0.4$) to orthorhombic ($Pbnm$; $z\geqslant 0.4$) ones. With further decreasing W, the AF state around $x=0.5$ is replaced by the charge-ordered insulating (COI) state. The spin structure in the COI state is a rather complicated one, with the $4\times4\times2$ unit cell in the cubic perovskite setting (CE type).[15] In Fig. 5 thus obtained ground states for the doped manganites in the $x-z$ space are summarized. The most important message of the phase diagram is that the ground state changes from the FM state to the A-type AF state with hole doping beyond $x\sim 0.5$ nearly independent of z (or W). Near $x\approx 1/2$ and the small-W region, however, the COI state appears, reflecting the enhanced charge-ordering instability due to commensuration of the nominal hole concentration with the lattice periodicity. Here we should emphasize that the ground-state spin structure is of the layered type, and hence the state can be viewed as a two-dimensional (2D) FM state, while the usual FM state is viewed as a 3D FM state. With further increasing x, an insulating state appears, as exemplified in $La_{0.4}Sr_{0.6}MnO_3$ ($x=0.6$, $z=0.0$), which may correspond to the COI state observed in $La_{1-x}Ca_xMnO_3$.[5,7]

The key factor that realizes the AFM state is considered to be the anisotropy of the two e_g orbitals, i.e., the two-dimensional $d_{x^2-y^2}$ state and the one-dimensional $d_{3z^2-r^2}$ state. Reflecting the anisotropy of the e_g orbitals, the electron transfer integral t_{ij} between the i and j sites strongly depends not only on the orbital species but also on the relative direction $\vec{r}_j-\vec{r}_i$. For example, t_{ij} between the $d_{x^2-y^2}$ states at $\vec{r}_j=\vec{r}_i\pm\hat{x}$ $(\hat{y},\hat{z})$ is $3/4t_0$ $(3/4t_0,0)$, while t_{ij} between the $d_{3z^2-r^2}$ states at $\vec{r}_j=\vec{r}_i\pm\hat{x}(\hat{y})$ is $1/4t_0$ $(1/4t_0)$, where t_0 is defined as the transfer integral between the $d_{3z^2-r^2}$ states at $\vec{r}_j=\vec{r}_i\pm\hat{z}$. Therefore, the e_g-electron system gains the maximum kinetic energy when the $d_{x^2-y^2}$ orbitals form a pseudo-2D band. If such a pseudo-2D band was realized, the in-plane exchange interaction would be ferromagnetic mediated by the itinerant $d_{x^2-y^2}$ electrons (DE interaction), while the antiferromagnetic superexchange interaction should

dominate along the z direction because of negligible t_{ij} value. This can explain not only the layered-type antiferromagnetic spin structure but also the metallic conductivity. In fact, for $(La_{0.5}Nd_{0.5})_{0.5}Sr_{0.5}MnO_3$,[9] elongation of lattice constants a and b as well as shrinkage of c is observed below T_N, which is advantageous to the formation of the pseudo-2D band. With decreasing x (see Fig. 5), or with increasing temperature (see Fig. 4), the orbital-ordered ground state changes into the 3D FM state. The most probable origin that destroys the 2D $d_{x^2-y^2}$ band is the JT instability inherent to the Mn^{3+} (d_4) ions, which lifts the degeneracy of the e_g orbitals and stabilizes the one-dimensional $d_{3z^2-r^2}$ state.

The A-type AF state, or the AFM state, is the fundamental ground state for the DE model with degenerated e_g orbital. Quite recently, Maezono *et al.*[16] have calculated a global phase diagram for the DE model explicitly taking account of the degeneracy of the e_g orbital and the anisotropy of the transfer integral in the mean-field approxmation. They observed a crossover of the ground state at around $x \sim 0.3$ from the ferromagnetic spin state to A-type AF spin state with the $d_{x^2-y^2}$ orbital structure, which shows excellent agreement with the experimentally derived phase diagram. The stabilization of the ferromagnetic state in the low x has been attributed to the superexchange interaction between the degenerated e_g orbitals. In an actual system, however, there exists the JT instability of the MnO_6 octahedra, which also favors the 3D FM state. The novel A-type state seems to be a fundamental ground state even for the doped manganites with the layered structure. Battle *et al.*[17] have reported a layered-type AF state for $NdSr_2Mn_2O_7$ ($x=0.50$) and $Nd_{1.1}Sr_{1.9}Mn_2O_7$ ($x=0.45$). We have measured the resistivity for the melt-grown single crystals of these antiferromagnetic manganites, and found that the AF state is highly conductive. Study along this trend is now in progress and will be published in a separate paper.

In conclusion, we have investigated the electronic and magnetic properties for $R_{1-x}Sr_xMnO_3$ ($R=La_{1-z}Nd_z$) by changing the nominal hole concentration x and the one-electron bandwidth W (or z). We have observed transformation of the ground state from the ferromagnetic metallic (FM) to the antiferromagnetic metallic (AFM) state with x beyond ~ 0.5. We propose that the AFM state is observed due to the formation of a pseudo-2D $d_{x^2-y^2}$ band. Our observation indicates that the e_g-orbital degree of freedom plays a crucial role in the ground state electronic structure for doped manganites.

The authors are grateful to Y. Endo, S. Ishihara, H. Kuwahara, and Y. Tokura for fruitful discussion and also to T. Inami for his help in the analysis of the neutron powder profiles. This work was supported by a Grant-In-Aid for Scientific Research from the Ministry of Education, Science and Culture, Japan and also from the Research Foundation for Materials Science.

*Author to whom correspondence should be addressed.

[1] For example, S. Jin, T. H. Tiefel, M. McCormack, R. Fastnacht, R. Ramesh, and L. H. Chen, Science **264**, 13 (1994).

[2] P. W. Anderson and H. Hasagawa, Phys. Rev. **100**, 675 (1955).

[3] P.-G. de Gennes, Phys. Rev. **118**, 141 (1960).

[4] N. Furukawa, J. Phys. Soc. Jpn. **63**, 3214 (1994); **64**, 2734 (1995); **64**, 2754 (1995); **64**, 3164 (1995).

[5] P. Schiffer, A. P. Ramirez, W. Bao, and S.-W. Cheong, Phys. Rev. Lett. **75**, 3336 (1995).

[6] A. J. Millis, P. B. Littlewood, and B. I. Shraiman, Phys. Rev. Lett. **74**, 5144 (1994); **77**, 175 (1996).

[7] A. P. Ramirez, P. Shiffer, S.-W. Cheong, C. H. Chen, W. Bao, T. T. M. Palstra, P. L. Gammel, D. J. Bishop, and B. Zegarski, Phys. Rev. Lett. **76**, 3188 (1996).

[8] H. Kawano, R. Kajimoto, H. Yoshizawa, Y. Tomioka, H. Kuwahara, and Y. Tokura, Phys. Rev. Lett. **78**, 4253 (1997).

[9] Y. Moritomo, H. Kuwahara, Y. Tomioka, and Y. Tokura, Phys. Rev. B **55**, 7549 (1997).

[10] F. Izumi, in *The Rietveld Method*, edited by R. A. Young (Oxford University Press, Oxford, 1993), Chap. 13; Y.-I. Kim and F. Izumi, J. Ceram. Soc. Jpn. **102**, 401 (1994).

[11] Outer side of the crystal ingot of $La_{0.46}Sr_{0.54}MnO_3$ is ferromagnetic possibly due to the reduced Sr concenration, which makes the Rietvelt refinement of the powder pattern difficult.

[12] Low-temperature resistivity measurement indicates that $Nd_{0.45}Sr_{0.55}MnO_3$ is an anisotropic metal with finite conductivity at zero temperature [H. Kuwahara *et al.* (unpublished)].

[13] A. Urushibara, Y. Moritomo, T. Arima, A. Asamitsu, G. Kido, and Y. Tokura, Phys. Rev. B **51**, 14 103 (1995).

[14] Y. Tomioka, A. Asamitsu, Y. Moritomo, H. Kuwahara, and Y. Tokura, Phys. Rev. Lett. **74**, 5108 (1995).

[15] E. O. Wollan and W. C. Koehler, Phys. Rev. **100**, 545 (1955).

[16] R. Maezono, S. Ishihara, and N. Nagaosa (unpublished).

[17] P. D. Battle, M. A. Green, N. S. Laskey, J. E. Millburn, P. G. Radaelli, M. J. Rosseinsky, S. P. Sullivan, and J. F. Vente, Phys. Rev. B **54**, 15 967 (1996).